High Power Laser Science and Engineering, (2018), Vol. 6, e26, 6 pages.

doi:10.1017/hpl.2018.16

Hexagonal boron nitride nanosheets incorporated antireflective silica coating with enhanced laser-induced damage threshold

Jing Wang[1,3,4], Chunhong Li[2], Wenjie Hu[3], Wei Han[2], Qihua Zhu[2], and Yao Xu[3]

[1]*Institute of Coal Chemistry, Chinese Academy of Sciences, Taiyuan 030001, China*

[2]*Research Center of Laser Fusion, China Academy of Engineering Physics, Mianyang 621900, China*

[3]*State Key Laboratory of Transient Optics and Photonics, Xi'an Institute of Optics and Precision Mechanics, Chinese Academy of Sciences, Xi'an 710119, China*

[4]*University of Chinese Academy of Sciences, Beijing 100049, China*

(Received 30 November 2017; revised 2 January 2018; accepted 7 March 2018)

Abstract

Boron nitride (BN) nanosheets incorporated silica antireflective (AR) coating was successfully prepared on fused silica substrate to improve the antilaser-damage ability of transmissive optics used in high-power laser systems. The BN nanosheets were obtained by urea assisted solid exfoliation, and then incorporated into basic-catalyzed silica sols without any further treatment. The transmission electron microscope (TEM) images indicated that the BN nanosheets generally consisted of 2–10 layers. The antireflective BN/SiO_2 coating exhibited excellent transmittance as high as 99.89% at 351 nm wavelength on fused silica substrate. The thermal conductivity 0.135 $W \cdot m^{-1} \cdot K^{-1}$ of the BN/SiO_2 coating with 10% BN addition was about 23% higher than 0.11 $W \cdot m^{-1} \cdot K^{-1}$ of the pure SiO_2 AR coating. The laser-induced damage threshold (LIDT) of that BN/SiO_2 coating is also 23.1% higher than that of pure SiO_2 AR coating. This research provides a potential application of BN/SiO_2 coatings in high-power laser systems.

Keywords: hexagonal boron nitride; laser-induced damage; silica antireflective coating; thermal conductivity

1. Introduction

Antireflective (AR) coating is an important type of optical coating applied to the surface of transparent optical elements to reduce reflection. In high-power laser systems, laser-induced damage of the optical coating is the most important factor that limits the further development of high-power laser[1]. Low laser-induced damage threshold (LIDT) not only reduces the laser beam quality, but leads to explosion of optical elements in vacuum. More and more attention is being paid to enhance LIDT of AR coating with the increase of laser power density. For this end, it is necessary to improve the surface quality of substrate and the interface energy diffusion between coating and substrate. The most frequently used methods for polishing substrate include ultrasonic cleaning, fine abrasive liquid polishing and super-polishing[2–4]. On the other hand, the current experimental results indicate that microdefect and absorption of the coating are the major factors that influence the quality of coating. To reduce microdefect density and absorption, and improve LIDT of coating, researchers have developed many methods, such as laser conditioning, ion post-treatment[5], effective cleaning process[6], modifying sols[7] and maintaining pressures[8] and temperature during deposition[9]. Silica AR coatings prepared by the sol–gel method have been widely used in high-power laser systems owing to its excellent optical performance, low cost, thermal mechanical properties and relatively high LIDT[10–13]. The common method of improving the quality of AR coating is to modify silica sol with polyvinyl butyral (PVB)[14] or polyvinylpyrrolidone (PVP)[15]. However, the addition of PVB and PVP into the silica sol decreases the porosity of coating, therefore, the refractive index of coating increases and the transmittance of coating decreases to 98%. Moreover, both of the methods are complex, and the thermal treatment of coating is needed. Hexagonal boron nitride (h-BN), a graphite-like inorganic compound composed of boron and nitrogen atoms in a hexagonal arrangement, has got recent attention[16, 17]. Combining the high thermal

Correspondence to: Y. Xu, State Key Laboratory of Transient Optics and Photonics, Xi'an Institute of Optics and Precision Mechanics, Chinese Academy of Sciences, Xi'an 710119, China. Email: xuyao@opt.ac.cn

conductivity (~280 $W \cdot m^{-1} \cdot K^{-1}$ in plane) and excellent electrical insulation, BN is a promising filler to enhance the thermal conductivity and retain the insulation of materials[18]. In addition, it is also noted that BN nanosheets exhibit high optical transmittance in ultraviolet, visible and near-infrared bands[19]. In recent years, many efforts have been made to fabricate low cost and high activity materials by incorporating silicon with BN[20, 21]. If BN nanosheets can be combined with silica coating, they may create a high LIDT AR coating.

2. Working principle

In this paper, BN/SiO_2 AR coating was successfully prepared by BN-incorporated SiO_2 sol. First, the BN nanosheets suspension was prepared by urea assisted solid exfoliation. Hexagonal boron nitride (Sinopharm Chemical, 98%) and urea (Sinopharm Chemical, 99.0%) were mixed in an agate milling container with the mass ratio of 1:60 and milled at a rotation speed of 600 $r \cdot min^{-1}$ for 48 h at room temperature. After ball milling, urea was removed through dialysis with deionized water for several times. In this process, few-layer BN nanosheets can readily be dispersed in water with sonication. After the water was evaporated, the solid product was redissolved in ethanol (Sinopharm Chemical, 99.7%), forming homogeneous BN nanosheets ethanol suspension. The concentration of BN nanosheets ethanol suspension was 0.2 $mg \cdot mL^{-1}$. The SiO_2 sol was prepared using tetraethyl orthosilicate (TEOS, ACROS, 98%) as precursor, ammonia (Sinopharm Chemical, 25%–28%) as catalyst and ethanol as solvent. The final molar ratio of SiO_2 sol was TEOS/ammonia/H_2O/ethanol = 1:0.57:2.45:38. The SiO_2 sol was stirred for 24 h and then aged for more than 7 days at room temperature. The BN/SiO_2 sols were prepared by adding BN nanosheets ethanol suspension into SiO_2 sol to form a mixture with 10wt% or 20wt% of BN nanosheets ethanol suspension. Then the BN/SiO_2 sols were sonicated for 20 min at room temperature. The final sols were accordingly marked as 10wt% BN/SiO_2 sol and 20wt% BN/SiO_2 sol, the concentration of BN nanosheets was 0.02 $mg \cdot mL^{-1}$ in 10wt% BN/SiO_2 sol and 0.04 $mg \cdot mL^{-1}$ in 20wt% BN/SiO_2 sol. The BN/SiO_2 AR coatings were deposited via dip-coating on well-polished and well-cleaned fused silica (Heraeus 312) substrates which were named SiO_2 coating, 10wt% BN/SiO_2 coating and 20wt% BN/SiO_2 coating.

The exfoliation process assisted by urea generated functional amino groups at defective sites and edges of BN (002) planes that made the BN nanosheets suspension more stable[22]. The left inset of Figure 1(a) shows a milky appearance of BN nanosheets water suspension, the concentration up to 1.0 $mg \cdot mL^{-1}$. After replacing the water with ethanol, the BN nanosheets ethanol suspension was very stable over several months under ambient conditions in a sealed bottle. In the right inset of Figure 1(a), the BN nanosheets ethanol suspension displays an obvious Tyndall effect due to the light scattering by BN nanosheets. Figure 1(a) also shows the distinct absorption peak at 204 nm (6.08 eV) which is attributed to the intrinsic exciton absorption band of BN nanosheets. The structure of BN nanosheets was also investigated by X-ray diffraction (XRD, Bruker D2). As shown in Figure 1(b), five peaks can be observed at 26.4°, 41.4°, 43.5°, 49.0° and 54.6°, corresponding to the (002), (100), (101), (102) and (004) planes of h-BN. Clearly, the (002) and (004) diffraction peaks of BN nanosheets became much stronger compared with the (100), (101), (102) peaks, which might be attributed to the enhanced exposure of (002) and (004) planes upon exfoliation, indicating BN nanosheets were peeled off along the (002) and (004) planes without considerable destroy of crystalline structure. The morphology of BN nanosheets was tested by a transmission electron microscope (HRTEM, JEOL-2100). TEM image of BN nanosheets shows that the BN nanosheets were flat and quite thin and the lateral sizes were 500–1000 nm, suggesting that the BN nanosheets remain intact and are not broken down by ball exfoliation. From Figure 1(d), HRTEM image at the edges of BN nanosheets clearly shows the thicknesses of BN nanosheets were significantly reduced. The layer numbers of obtained BN nanosheets were 2–10, corresponding to the thickness of 1–4 nm. Incorporation of such thinner BN nanosheets into SiO_2 sols may have little influence on transmittance of SiO_2 AR coating.

The detailed dispersion of BN nanosheets in the BN/SiO_2 coating was characterized by Raman spectroscopy mapping technology (RAMANforce, Nanophoton Corporation) at a laser wavelength of 532 nm. Figure 2(a) shows the Raman mapping of 10wt% BN/SiO_2 coating and the green dots display the locations of BN nanosheets and indicates the BN nanosheets are uniformly distributed in the BN/SiO_2 coating. Figure 2(b) shows the Raman spectrum of area (1) in the mapping image. Only the typical peak of E_{2g} mode can be found at ~1366 cm^{-1}, indicating few-layer BN nanosheets were present in the BN/SiO_2 coating. Figure 2(c) shows the TEM image of 10wt% BN/SiO_2 sol, in which the SiO_2 particles were uniformly distributed on the BN nanosheets. That is consistent with the Raman-mapping result. The inset in Figure 2(c) shows the uniform particle size distribution of SiO_2 particles with diameter of about 10 nm, which determined the antireflection at 351 nm wavelength of BN/SiO_2 coating[23]. Figure 2(d) shows the HRTEM image of the 10wt% BN/SiO_2 sol, in which the BN nanosheets can be clearly seen between several SiO_2 particles.

The surface morphology of BN/SiO_2 coating was confirmed by atomic-force microscopy (AFM) (Innova, Bruker). In order to obtain the more precise roughness values, each coating was measured at ten points of random selection and finally the average was taken. Figure 3 shows the AFM images of bare fused silica substrate, SiO_2 coating, 10wt% BN/SiO_2 coating and 20wt% BN/SiO_2 coating which were

https://doi.org/10.1017/hpl.2018.16 Published online by Cambridge University Press

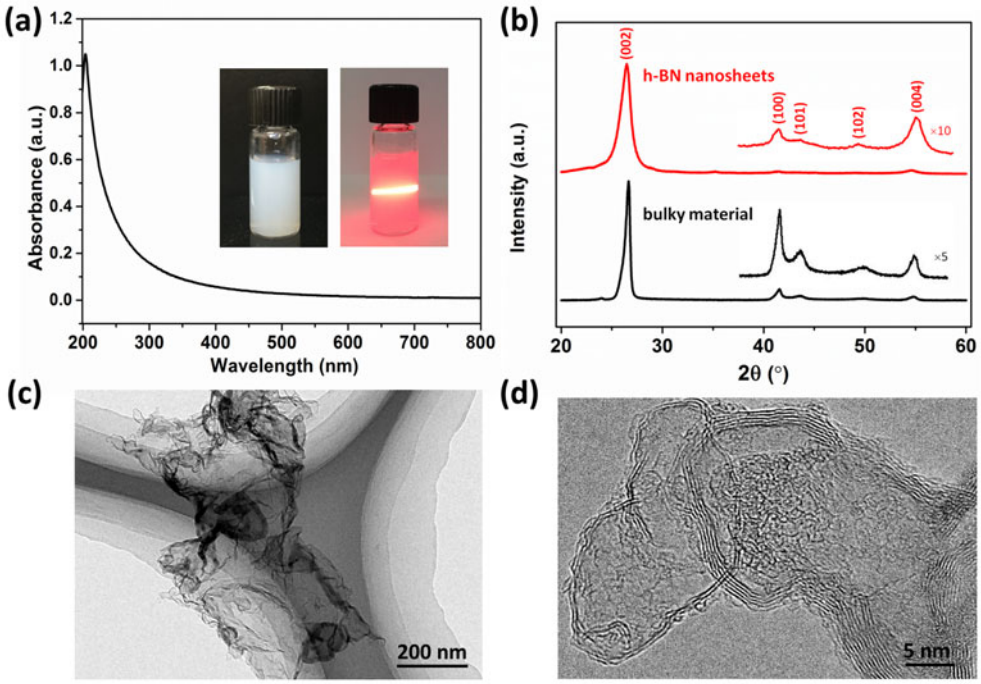

Figure 1. (a) Optical absorption of BN nanosheets dispersion in ethanol. Inset: photographs of BN nanosheets dispersion in water (left) and ethanol (right). (b) XRD patterns of BN nanosheets we used here and h-BN bulky material. Inset: the curves in the region of 37°–57°. (c) TEM and (d) HRTEM images of BN nanosheets.

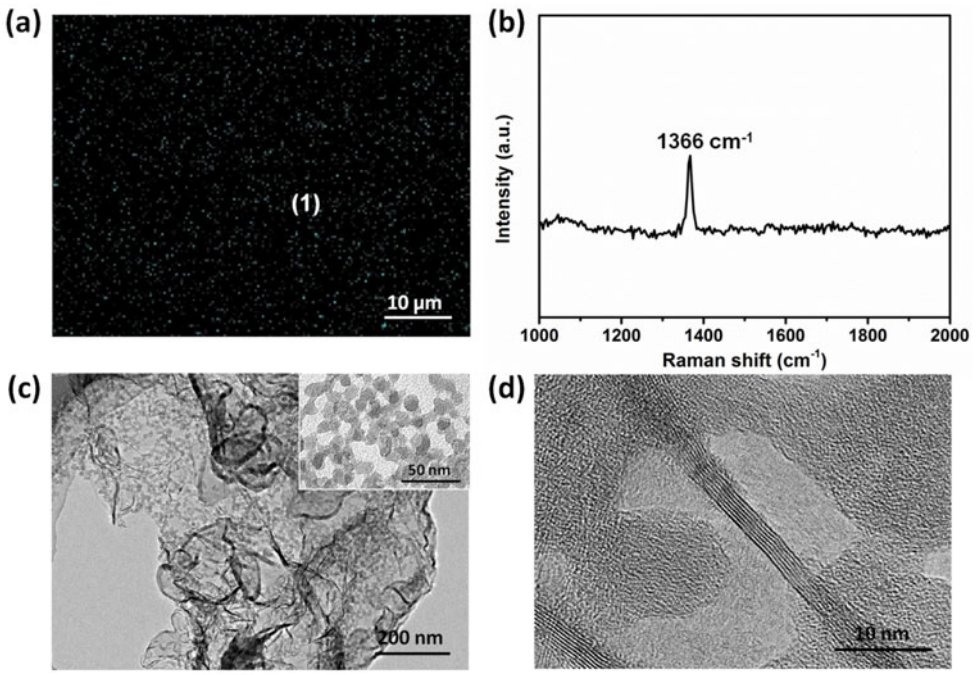

Figure 2. (a) Raman-mapping image of 10wt% BN/SiO_2 coating: green dots are BN nanosheets. (b) The Raman spectrum of area (1) in the mapping. (c) TEM image of 10wt% BN/SiO_2 sol. Inset: TEM image of SiO_2 particles. (d) HRTEM image of BN nanosheets in the 10wt% BN/SiO_2 sol.

https://doi.org/10.1017/hpl.2018.16 Published online by Cambridge University Press

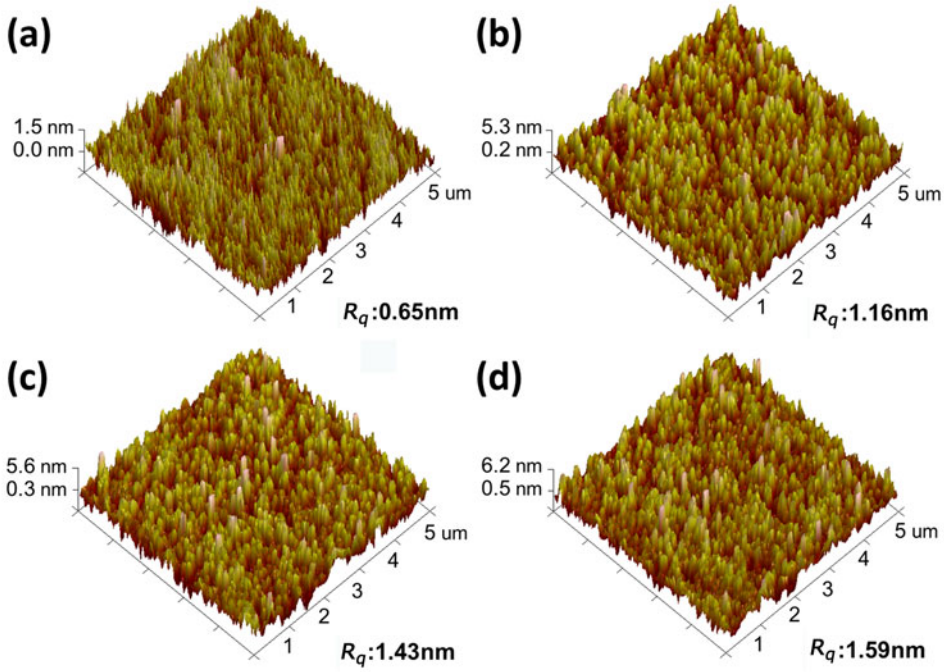

Figure 3. AFM images of (a) bare fused silica substrate, (b) SiO_2 coating, (c) 10wt% BN/SiO_2 coating and (d) 20wt% BN/SiO_2 coating.

randomly selected from obtained images. The root-mean-square roughness (R_q) values of coatings were calculated using the AFM images. As BN nanosheets were incorporated into SiO_2 sols, the R_q values show a small increase for 10wt% BN/SiO_2 coating and 20wt% BN/SiO_2 coating. Because the R_q values of all the BN/SiO_2 coatings were less than 2 nm, the surface scattering of coating was small enough to avoid additional decrease in transmittance. Meanwhile, there is little difference in R_q between 10wt% BN/SiO_2 coating and 20wt% BN/SiO_2 coating, which indicates the lateral sizes and thicknesses of BN nanosheets were suitable for preparing BN/SiO_2 AR coating. Both AFM and TEM results were mutually complementary and offered a very detailed analysis of BN/SiO_2 coatings.

In order to investigate the optical property of BN/SiO_2 AR coating, fused silica substrates were coated by dipping into the SiO_2 sol, 10wt% BN/SiO_2 sol and 20wt% BN/SiO_2 sol. The refractive index and thickness of AR coatings were calculated using a spectroscopic ellipsometer (SC620, Sanco) at 60° incidence, and listed in Table 1. The optical thickness of coating was controlled to match the desired antireflective wavelength 351 nm by adjusting the dipping speed. The optical transmittance results were measured by a UV–Vis–NIR spectrometer (U-4100, Hitachi) in the wavelength range from 200 to 800 nm. Figure 4 shows the transmittance spectra of SiO_2 coating, 10wt% BN/SiO_2 coating and 20wt% BN/SiO_2 coating. As shown in Table 1, the maximum transmittances of SiO_2 coating, 10wt% BN/SiO_2 coating and 20wt% BN/SiO_2 coating are all over 99.8% at 351 nm, which is an excellent antireflective performance for applying in high-power laser systems. Almost the same transmittance of coatings is mainly due to the high optical transmittance of BN nanosheets in ultraviolet, visible and near-infrared bands and the small concentration of BN nanosheets in sol which was too small to affect the transmittance of coating. The digital image of 10wt% BN/SiO_2 coating on fused silica substrate is shown in Figure 4, which indicates a significantly improved transmittance of BN/SiO_2 coating.

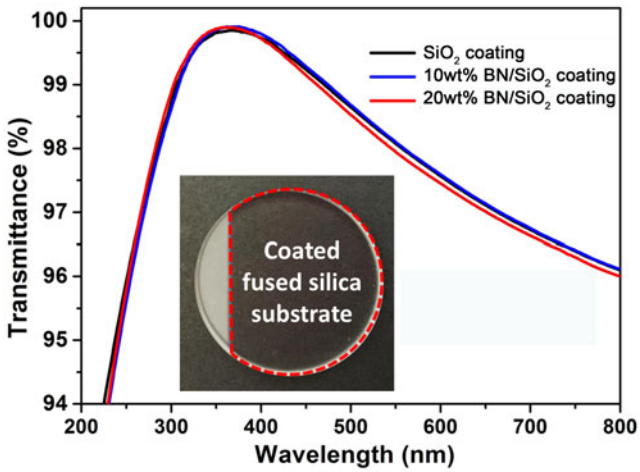

Figure 4. Transmittance of SiO_2 coating, 10wt% BN/SiO_2 coating and 20wt% BN/SiO_2 coating. The inset is the photograph of 10wt% BN/SiO_2 coating on fused silica substrate to show the high transmittance.

Laser-induced damage threshold test was performed via the 'R-on-1' mode according to ISO standard 11254-2: 2000,

https://doi.org/10.1017/hpl.2018.16 Published online by Cambridge University Press

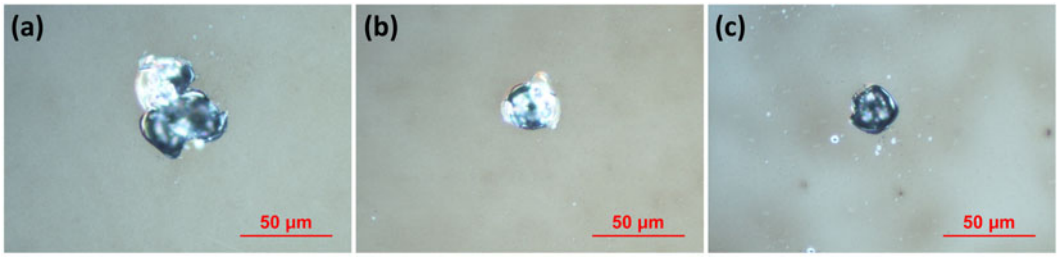

Figure 5. Laser-induced damage morphologies of AR coatings (a) SiO_2 coating, (b) 10wt% BN/SiO_2 coating and (c) 20wt% BN/SiO_2 coating.

Table 1. Optical parameters of BN/SiO_2 coatings with various BN nanosheets mass ratios.

Sample	n_f	Thickness (nm)	T_{max} (%)	R_q (nm)	Average LIDT (J cm^{-2})
Bare fused silica substrate	1.46	–	93.56	0.514	8.69
SiO_2 coating	1.25	73	99.84	2.597	8.92
10wt% BN/SiO_2 coating	1.24	75	99.89	3.740	10.98
20wt% BN/SiO_2 coating	1.24	74	99.92	3.638	8.96

n_f is the refractive index of coating; T_{max} is the maximum transmittance at 351 nm; R_q is the root-mean-square roughness value of coating; LIDT means laser-induced damage threshold with 6.60 ns pulse of 351 nm laser.

using a 351 nm pulse laser with a pulse width of 6.6 ns and the laser spot area of 1.02 mm^2. The LIDT data of coatings are shown in Table 1. There was a small increase in the threshold from 8.69 to 8.92 J · cm^{-2} as the traditional SiO_2 coating was deposited on the fused silica substrate. Under laser irradiation, the coating was destroyed when the surface temperature increased to the melting point after the laser energy was absorbed by coating. The LIDT result of 10wt% BN/SiO_2 coating is significantly higher than that of bare SiO_2 coating on fused silica substrate, especially the 10wt% BN/SiO_2 coating shows 23.1% increase of LIDT without any other treatment. The enhanced LIDT of 20wt% BN/SiO_2 coating is only 8.96 J · cm^{-2}, which is much smaller than that of 10wt% BN/SiO_2 coating.

In addition to the LIDT, damage morphology of coating was tested to analyze the laser damage mechanism of coating. Figure 5 shows the laser-induced damage morphology of SiO_2 coating, 10wt% BN/SiO_2 coating and 20wt% BN/SiO_2 coating. As can be seen from Figures 5(a) and 5(b), the damage area of 10wt% BN/SiO_2 coating is smaller than that of the bare SiO_2 coating, which indicates the 10wt% BN/SiO_2 coating suffered the milder damage[14]. Seen from Figure 5(c), there are some tiny damage dots on the surface of 20wt% BN/SiO_2 coating. This may be attributed to plenty of BN nanosheets in coating, the more BN nanosheets in coating, the worse adhesion of coating would be.

As an excellent thermally conductive material, BN has been used to prepare electron-insulative and thermally conductive composites. Sato *et al.*[24] prepared an h-BN/polyimide composite film with high thermal conductivity up to 7 W · m^{-1} · K^{-1}, in which the active edge planes of h-BN filler most probably interacted chemically with the surrounding polyimide matrix. The enhanced interactions resulted in fewer flaws, coherent interfaces and minimal interfacial phonon scattering. Zhou and co-workers[25] reported a thermally conductive silicone rubber used BN powder as conductive fillers. The inclusion of BN increases both thermal conductivity and thermal stability, while decreases the coefficient of thermal expansion. Cho *et al.*[26] reported a facile technique that modified BN nanosheets with iron oxides in order to fabricate highly oriented polysiloxane/BN nanosheet composite films. The thermal property of polysiloxane/BN nanosheet composite film was determined by the orientation of BN, and the thermal conductivity of composite film was enhanced by 20 times after addition of BN nanosheets.

Here, BN nanosheets played an important role in enhancing the diffusion of heat because of its extremely high in-plane thermal conductivity and insulation, but low coefficient of thermal expansion and superior thermal stability[27, 28]. Because traditional basic silica coating was porous, the absorbed thermal energy cannot effectively transfer through the separated silica particles and the surrounding voids. BN nanosheets have good thermal conductivity, so the thermal conductivity of BN/SiO_2 coating must be higher than that of the traditional basic silica coating. With the laser radiation, the BN/SiO_2 coating has good slow-release ability to the local strain caused by the absorbed laser energy. A laser thermal conductivity testing instrument (NanoTR, NETZSCH) was used to evaluate the thermal conductivity of SiO_2 coating and 10wt% BN/SiO_2 coating. The thermal conductivity coefficient of 10wt% BN/SiO_2 coating is 0.135 W · m^{-1} · K^{-1}, 23% higher than 0.110 W · m^{-1} · K^{-1} of bare SiO_2 coating, which was consistent with the increased LIDT.

In summary, the antireflective BN/SiO_2 coatings have been successfully prepared through incorporating BN nanosheets

https://doi.org/10.1017/hpl.2018.16 Published online by Cambridge University Press

into traditional basic silica sol without any additional treatment. The BN/SiO_2 coatings revealed very promising antireflective properties at 351 nm and also enhanced LIDT performance. This is a good candidate for the future application of AR coating in optical components for a high-power laser system. In contrast with other modifying silica sol methods, this work has very low cost and simple process. By optimizing the content of BN nanosheets, coating material, and other design parameters, the antilaser-damage ability may be further enhanced.

Acknowledgement

This work was supported by National Natural Science Foundation of China (Nos. U1530148 and 61605188).

References

1. N. Bloembergen, Appl. Opt. **12**, 661 (1973).
2. B. Bertussi, J.-Y. Natoli, and M. Commandre, Opt. Commun. **242**, 227 (2004).
3. J. A. Menapace, B. Penetrante, D. Golini, A. Slomba, P. E. Miller, T. Parham, M. Nichols, and J. Peterson, Proc. SPIE **4679**, 56 (2002).
4. F. Shi, Y. Shu, Y.-F. Dai, X.-Q. Peng, and S.-Y. Li, Opt. Eng. **52**, 9 (2013).
5. D.-P. Zhang, P. Fan, X.-M. Cai, J.-D. Shao, and Z.-X. Fan, Proc. SPIE **6722**, 67221Q (2007).
6. E. S. Field, J. C. Bellum, and D. E. Kletecka, Proc. SPIE **9983**, 998314 (2016).
7. B. Shen, H.-Y. Li, L.-Y. Zhao, and Y.-X. Tang, Proc. SPIE **10255**, 102550W (2017).
8. M.-Q. Zhan, T.-Y. Tan, D.-W. Zhang, H.-B. He, J.-D. Shao, and Z.-X. Fan, Proc. SPIE **5774**, 365 (2004).
9. E. S. Field, J. C. Bellum, and D. E. Kletecka, Proc. SPIE **9632**, 963219 (2015).
10. Y. Xu, D. Wu, Y.-H. Sun, Z.-X. Huang, X.-D. Jiang, X.-F. Wei, Z.-H. Li, B.-Z. Dong, and Z.-H. Wu, Appl. Opt. **44**, 527 (2005).
11. T. I. Suratwala, M. L. Hanna, E. L. Miller, P. K. Whitman, I. M. Thomas, P. R. Ehrmann, R. S. Maxwell, and A. K. Burnham, J. Non-Cryst. Solids. **316**, 349 (2003).
12. A. L. Rigatti, Proc. SPIE **5647**, 136 (2005).
13. X.-G. Li, L.-P. Zou, G.-M. Wu, and J. Shen, Opt. Mater. Express **4**, 2478 (2014).
14. F.-T. Chi, L.-H. Yan, H.-B. Lv, C.-C. Wang, and X.-D. Yuan, Thin Solid Films **519**, 2483 (2011).
15. L. Zhang, Y. Xu, D. Wu, Y.-H. Sun, X.-D. Jiang, and X.-F. Wei, Opt. Laser Technol. **40**, 282 (2008).
16. Y. Wang, Z.-X. Shi, and J. Yin, J. Mater. Chem. **21**, 11371 (2011).
17. L. Liu, Y. P. Feng, and Z. X. Shen, Phys. Rev. B **68**, 104102 (2003).
18. J.-W. Gu, Q.-Y. Zhang, J. Dang, and C. Xie, Polym. Adv. Technol. **23**, 1025 (2012).
19. A. B. Abdellaoui, B. Bouchikhi, and O. Baehr, Mater. Sci. Eng. B **47**, 257 (1997).
20. J. D. Ferguson, A. W. Weimer, and S. M. George, Chem. Mater. **12**, 3472 (2000).
21. S. Lin, X.-X. Ye, and J. Huang, Phys. Chem. Chem. Phys. **17**, 888 (2015).
22. W.-W. Lei, V. N. Mochalin, D. Liu, S. Qin, Y. Gogotsi, and Y. Chen, Nat. Commun. **6**, 8 (2015).
23. N. Bazin, J. E. Andrew, and H. A. Mcinnes, J. Sol-Gel Sci. Technol. **13**, 757 (1998).
24. K. Sato, H. Horibe, T. Shirai, Y. Hotta, H. Nakano, H. Nagai, K. Mitsuishi, and K. Watari, J. Mater. Chem. **20**, 2749 (2010).
25. W.-Y. Zhou, S.-H. Qi, H.-Z. Zhao, and N.-L. Liu, Polym. Compos. **28**, 23 (2007).
26. H.-B. Cho, Y. Tokoi, S. Tanaka, H. Suematsu, T. Suzuki, W.-H. Jiang, K. Niihara, and T. Nakayama, Compos. Sci. Technol. **71**, 1046 (2011).
27. W.-Y. Zhou, S.-H. Qi, Q.-L. An, H.-Z. Zhao, and N.-L. Liu, Mater. Res. Bull. **42**, 1863 (2007).
28. D. S. Williams, J. Appl. Phys. **57**, 2340 (1985).

https://doi.org/10.1017/hpl.2018.16 Published online by Cambridge University Press